Journal of Surface Engineered Materials and Advanced Technology, 2024, 14, 1-14
https://www.scirp.org/journal/jsemat
ISSN Online: 2161-489X
ISSN Print: 2161-4881

Solid Particle Erosion of AISI 304 SS Caused by Alumina Particles

Juan Rodrigo Laguna-Camacho[1*], Celia María Calderón-Ramón[1], Víctor Velázquez-Martínez[1], Javier Calderón-Sánchez[1], Gabriel Juárez-Morales[1], Cristóbal Cortez-Domínguez[1], Jorge Alberto Chagoya-Ramírez[1], Jesús Enrique López-Calderón[1], Paul Ramírez-Sánchez[1], Silvia Marina Sánchez-Yáñez[2], Héctor Daniel López-Calderón[3], Antonio de Jesús Cárdenas-Hernández[1]

[1]Faculty of Electrical and Mechanical Engineering, Universidad Veracruzana, Poza Rica, Veracruz, Mexico
[2]Facultad de Ciencias Biológicas y Agropecuarias, Universidad Veracruzana, Tuxpan, Veracruz, Mexico
[3]Facultad de Biología, Universidad Veracruzana, Xalapa, Veracruz, Mexico
Email: *juanrodrigo.laguna@gmail.com

How to cite this paper: Laguna-Camacho, J.R., Calderón-Ramón, C.M., Velázquez-Martínez, V., Calderón-Sánchez, J., Juárez-Morales, G., Cortez-Domínguez, C., Chagoya-Ramírez, J.A., López-Calderón, J.E., Ramírez-Sánchez, P., Sánchez-Yáñez, S.M., López-Calderón, H.D. and Cárdenas-Hernández, A. de J. (2024) Solid Particle Erosion of AISI 304 SS Caused by Alumina Particles. *Journal of Surface Engineered Materials and Advanced Technology*, **14**, 1-14.
https://doi.org/10.4236/jsemat.2024.141001

Received: January 1, 2024
Accepted: January 28, 2024
Published: January 31, 2024

Abstract

This research work was carried out with the aim of continuing to expand knowledge on the behaviour of AISI 304 stainless steel against solid particle erosion. In this particular case, the steel was subjected to the impact of alumina particles, which are hard abrasives with irregular and angular shapes. Different characterization techniques were applied to gain a better understanding of alumina. For instance, particle size distribution was obtained using the Analysette 28 Image Sizer and the particle size was between 300 - 400 μm. SEM and EDS analysis were used to know the morphology and chemical composition of both the abrasive particles and AISI 304 stainless steel. Additionally, mechanical properties values such as the hardness and Young's modulus of AISI 304 steel were attained using a Berkovich indenter (model TTX-NHT, CSM Instruments). On the other hand, two tests were carried out for each impact angle used, 30˚, 45˚, 60˚ and 90˚, with a particle velocity of 24 ± 2 m/s and an abrasive flow rate of 63 ± 0.5 g/min, employing a test rig based on ASTM G76-95 standard. SEM images using two detectors, Backscattered Electron Detector (BED) and Low Electron Detector (LED), were employed to identify the wear mechanisms on the AISI 304 eroded surfaces at 30˚ and 90˚. Finally, the erosion rates of AISI 304 compared to those results reached by AISI 1018 steel and AISI 420 stainless steel tested under identical conditions in previous works.

Keywords

Solid Particle Erosion, AISI 304 Stainless Steel, Alumina Particles, Wear

Mechanisms, Erosion Rates

1. Introduction

Solid particle erosion is a wear mode incurred by organic and inorganic particles of different hardness, size and shape (spherical and angular natures). Abrasive particles such as silicon carbide (SiC), aluminum oxide, alumina (Al_2O_3), steel grits, quartz sand, glass beads, ashes, walnut grits and others, have been used in several research works to show how the abrasive particles inflicted damage on surfaces. As these particles impinge on a surface, they immediately cause material removal. Wear mechanisms such as micro-cutting and micro-ploughing actions on the surfaces are commonly observed at low incident angles (30˚ and 45˚), whereas intense pitting, smeared wear debris or flattened lips are characteristics at higher incident angles (60˚ and 90˚). This wear type has been reported as a significant problem in different mechanical elements such as gas and steam turbine blades [1], bends, valves in bulk material handling applications, surfaces of chutes [2] and hoppers in food processing. In many of these mechanical components, steel alloys are employed due to their high strength, ductility, resilience and fracture toughness. For this reason, various studies related to solid particle erosion of steel alloys using diverse abrasive particles have been performed over the years. For instance, Morrison *et al.* [3] carried out a solid particle erosion study on AISI 304 stainless steel using aluminum oxide particles with different particle sizes to evaluate this parameter. The erosion rate results showed that the maximum erosion damage occurred at nearly 20˚, and as the particle size increased, the erosion wear amplified. However, with larger particles, there could be a saturation of the incoming and rebounding particles at high incident angles. An important finding was seen in SEM micrographs used to identify the wear mechanisms at different incidence angles that ranged from 10˚ to 90˚. The photographs showed that the wear mechanisms were quite similar at low and high impact angles, 20˚ and 90˚, which confirmed the possibility of a single wear mechanism occurring in ductile materials at any incident angle. The surface damage is mainly characterized by material displacement, shearing and smeared platelets. In some wear areas, cracks are observed on the surface. It concluded that a cumulative number of impacts could lead to plastic deformation of the material even when it had a high hardness. In addition, Foley & Levy [4] performed erosion testing on three steels, AISI 1020, AISI 304 and AISI 4340, in different heat-treated conditions employing alumina (Al_2O_3) particles with a size of 140 μm. The main finding in this research work was that the erosion resistance of the steels significantly increased as the ductility was higher. In these specific testing conditions, using heat treatments, mechanical properties such as hardness, strength, fracture toughness and impact strength were not such significant parameters in the erosion behavior of tested steels. With respect to AISI 304 in both, as-wrought and annealed conditions, this stainless

steel exhibited its maximum erosion resistance in the annealed condition which was an expected result due to the ductility of this material being higher at this particular state. This material presented a typical ductile behavior, reaching its maximum erosion rate at 30˚. On the other hand, the microstructure effect on the erosion resistance was analyzed and the results exhibited a higher erosion rate as the hardness of AISI 1020 steel in hot rolled and cold rolled conditions decreased at approximately 10 HRB, and a plot showed that as the hardness increased the erosion values reduced permanently up to 50 HRB. The results related to the elongation percentage and, hence, the ductility of the hot rolled samples played a significant role in considerably reducing erosion wear rates. In relation to the erosion behavior of AISI 4340 steel, it was tested using different heat treatments, tempered and spheroidized by annealing, and the results did not show significant differences among the erosion rates, however the spheroidized steel by annealing presented slightly better erosion resistance, it had a higher elongation percentage (higher ductility). The SEM micrographs showed that the platelet mechanism was consistent with all tested materials. It concluded that a higher ductility of the steels allowed the spreading of the kinetic energy transmitted by the erodent particles on all the sample geometry rather than concentrated in a single point. Therefore, the capacity of the ductile metals to deform plastically in a permanent form was a meaningful parameter to decrease the erosion damage on the surfaces. In addition, Tilly [5] presented erosion testing of metals and plastics. Materials such as aluminum, aluminum alloys, stainless steels and tool steels were tested. In this work, the particle size is considered as one of the most important parameters in erosion studies. The results showed that as the abrasive particle size increased, the erosion rate pronounced in a more intense way. Furthermore, this study mentioned that the erosion rates could decrease considerably with materials that have a greater tensile strength (higher ductility), which coincided with Foley & Levy [4]. Then, Goretta *et al.* [6] carried out a study comparing the erosion resistance of three different materials: C11000 copper, nickel and AISI 304 stainless steel. This study was conducted to determine the effects of work hardening, hardness and ductility on the erosion resistance of materials. The paper mentioned that erosion rates in different metals did not depend on a particular mechanical property. The most constant correlation to improve the erosion resistance of materials occurred as the material ductility increased. That was, if the material subject to erosion tests had a good ductility, then it would have a greater possibility of deforming and dissipating the energy transmitted by the impact of abrasive particles. The erosion results of the three materials were compared, and nickel was the material with the highest erosion resistance, with a more constant performance at all impact angles, whereas copper acquired higher erosion rates. Singh *et al.* [7] conducted erosion tests at room temperature to study the erosion behavior of three different stainless steels such as AISI 304, 316 and 410. In this work, three impact angles (30˚, 60˚ and 90˚) and two impact velocities (98 and 129 m/s) were used. Silicon carbide (density 3100 kg/m^3) was employed as erodent. The general shape

of the SiC particles was angular and their size was 160 μm. The results indicated that 410 stainless steel demonstrated the maximum erosion resistance compared to 304 and 316 stainless steels. The three stainless steels presented a ductile erosion behavior reaching their maximum erosion rate at oblique incident angles ($\alpha \geq 45^{\circ}$). In addition, the effect of particle velocity was analyzed and the results at all steels exhibited higher erosion rates as the particle velocities magnified. The wear mechanisms identified in the three stainless steels at 30˚ and 90˚, were the ploughing action with the lips or platelets formed at the end of the particle trajectories, micro-cutting and pitting damage were also identified. Finally, Shayler & Yee [8] also carried out research on the erosion of AISI 303 stainless steel targets using two types of erodent particles coming from pulverized fuel coal ashes (42 - 66 μm) and pressurized fluidized bed combustion ashes (2.3 μm). These abrasive particles were used because the authors had a special interest in the erosion problems caused by the fine ashes in the flue gases from coal combustion to drive gas turbines, in pressurized fluidized beds (PFBC). A sandblasting erosion rig and a wind tunnel erosion equipment were employed to conduct the tests. The test results showed that for large coal ash particles (42 - 66 μm), the erosion rates were of the same order of magnitude in both test facilities. On the other hand, the erosion rates of AISI 303 are influenced by the aerodynamic flow effects around the target for the PBFC coal ash particles, with an average size of 2.3 μm. This effect greatly reduced the erosion rates.

In this work, solid particle erosion tests on AISI 304 stainless steel were conducted. Both AISI 304 steel and alumina particles are characterized by using SEM to know their morphology. In addition, a nanoindentation technique was employed to obtain the hardness and Young's modulus of AISI 304. An erosion rig based on ASTM G76-95, was used to run the tests. With respect to the wear damage originated by alumina particles, it was possible to identify typical wear mechanisms in the SEM images, such as micro-cutting, micro-ploughing and pitting actions, scratches, displaced and flattened material on the damaged surfaces. The SEM photographs were taken by two detectors: Backscattered Electron Detector (BED), specifically employed to have a contrast of the surface images, making it possible to observe deep details of the surface topographies, and Low Electron Detector (LED). The total erosion wear rates obtained at all incident angles and compared to those reached by the other two steels, AISI 1018 and AISI 420 under these particular testing conditions.

2. Experimental Details

2.1. Specimens

The material used in the tests was AISI 304 austenitic stainless steel in the soft annealed condition (0.08% Wt. C, 3.02% Si, 9.89% Cr, 7.03% Ni, 79.98% Fe). In this particular case, the steel was heated uniformly to temperatures between 1038˚C - 1121˚C, and then cooled rapidly to get the annealing state. The sample dimensions were 50 mm × 25 mm and 3 mm in thickness. With respect to alumina

particles, SEM photographs show an irregular shape with different magnifications in Figures 1(a)-(b). The chemical composition of alumina erodent was obtained by Energy Dispersive X-ray analysis (EDS), Figure 1(c). In addition, particle size distribution was attained using the Analysette 28 ImageSizer and the alumina particles had a particle size between 300 - 400 μm. The alumina hardness was 1200 HV (as received) whereas AISI 304 steel had 254.79 HV with a standard deviation of 41.46 and the Young's modulus was 194.40 GPa with a standard deviation of 12.61 (after 15 measurements). The hardness and Young's modulus values were obtained using a Berkovich indenter (model TTX-NHT, CSM Instruments).

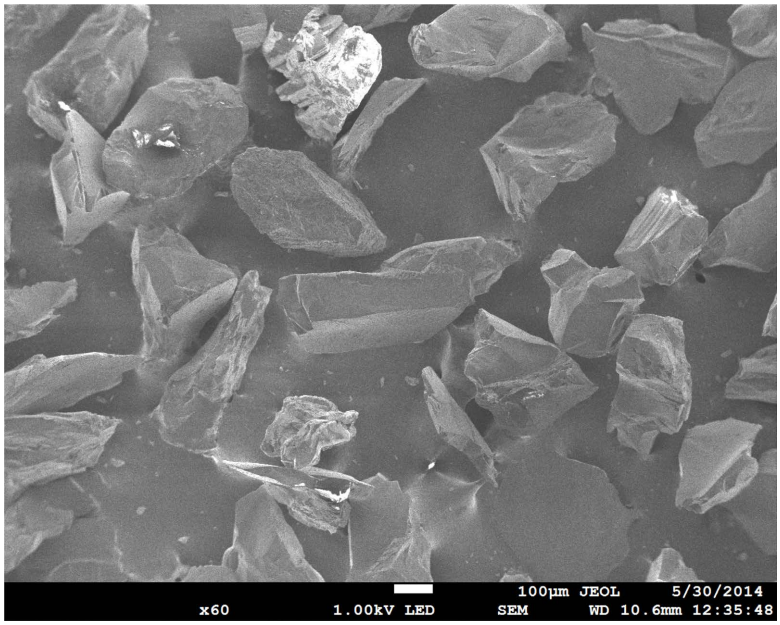

(a)

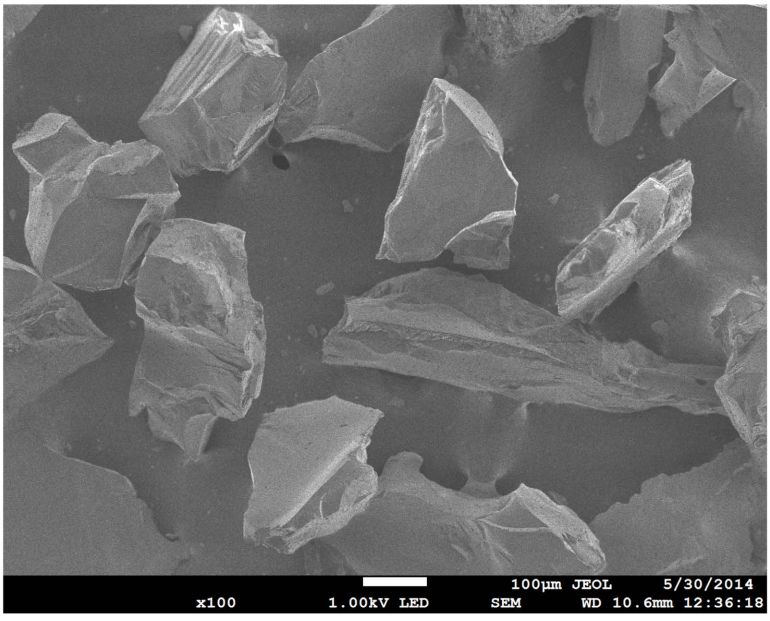

(b)

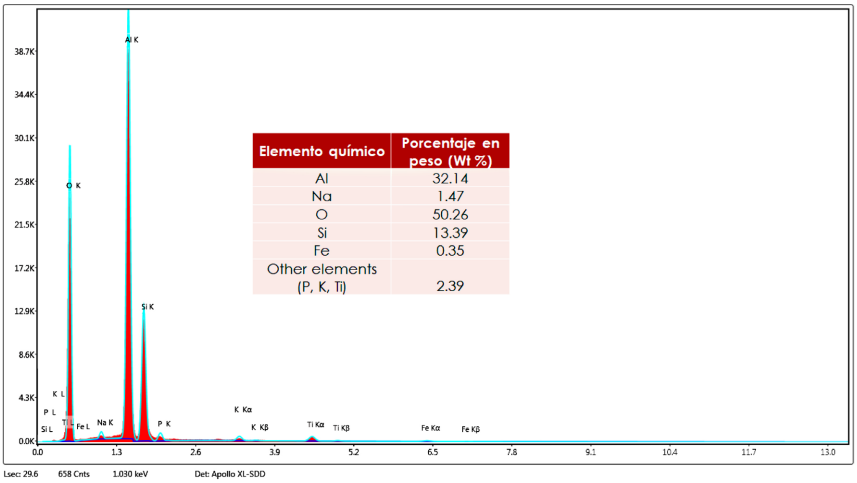

Elemento químico	Porcentaje en peso (Wt %)
Al	32.14
Na	1.47
O	50.26
Si	13.39
Fe	0.35
Other elements (P, K, Ti)	2.39

(c)

Figure 1. Morphology of the alumina particles (Al_2O_3). (a) 60×; (b) 100×; (c) EDS of alumina particles.

2.2. Test Procedure

The erosion tests were performed by using a common rig, based on that presented in ASTM G76-95 [9]. The schematic diagram of the rig was shown in different research works [10]. The material eroded by 10 min, although each sample was removed every 2 min to determine the mass loss. The impact angles used for the tests were 30˚, 45˚, 60˚ and 90˚. A particle velocity of 24 ± 2 m/s and an abrasive flow rate of 63 ± 0.5 g/min were employed to conduct the tests. In all of the tests, the specimens were located 10 mm from the end of the stainless steel nozzle. The nozzle dimensions were 4.7 mm internal diameter, 6.3 mm external diameter and 260 mm length. The room temperature was between 35˚C and 40˚C, due to the extreme weather in Poza Rica de Hidalgo, Veracruz, Mexico. The specimens were weighed using an analytical balance (with an accuracy of ± 0.0001 g) before the start of each test and removed every 2 min, cleaned by using acetone and weighed again to determine the mass loss amount. The micrographs of the eroded surfaces by alumina were acquired using SEM with two detectors, Backscattered Electron Detector (BED) and Low Electron Detector (LED) to identify the wear mechanisms.

3. Results and Discussion

3.1. Discussion of the Results

Erosion caused by alumina particles

The surface micrographs were obtained using a Scanning Electron Microscope (SEM), model Quanta 3D FEG (FEI). The erosion damage caused by alumina is characterized by high plastic deformation due to micro-cutting, micro-ploughing, irregular scratches and indentations on random positions at 30˚ (**Figures 2(a)-(d)**). Also, embedded fragments, a few pits and lifted lips or platelets occasioned by abrasive particles sliding on the surface, were observed. The BED detector allowed seeing clearly particle fragments (dark areas) **Figure 2(a)** and **Figure 2(c)**,

or wear debris embedded on the eroded surfaces. These wear mechanisms are quite typical of ductile materials such as AISI 304 steel. On the other hand, the LED detector obtained common SEM photographs of the eroded areas and the high material displacement observed in **Figure 2(b)** and **Figure 2(d)**.

In relation to the erosion damage at 90˚ (normal incidence), the surfaces showed darker areas (BED detector) which could be due to the intense pitting action filled by smeared or flattened wear debris (**Figure 3(a)** and **Figure 3(c)**) and also possible cracks identified employing LED detector (**Figure 3(b)** and **Figures 3(d)-(e)**). A quite common big pit was observed on the surface of AISI 304 steel and a possible alumina particle was clearly observed inside the void (**Figure 3(d)**). An unexpected wear mechanism presented at 90˚ (**Figure 3(e)**), is because a typical ploughing action formed on the surface, however it could occur by particles or particle fragments that impinged on the surface and rebounded with the nozzle and then slid again on the material surface causing this particular wear damage normally seen at low incident angles ($\alpha \geq 45^{\circ}$). These erosion modes are quite typical with hard abrasives and angular shapes such as aluminium oxide, silicon carbide, steel grit and quartz sand [3] [11]-[14].

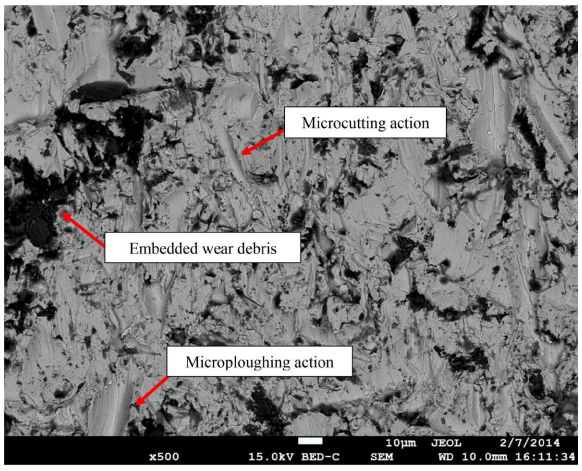

(a)

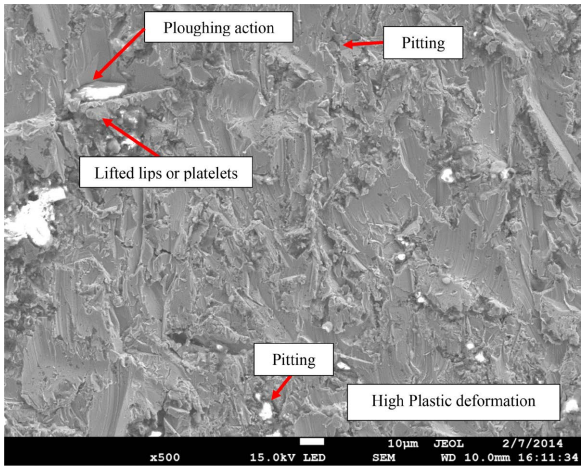

(b)

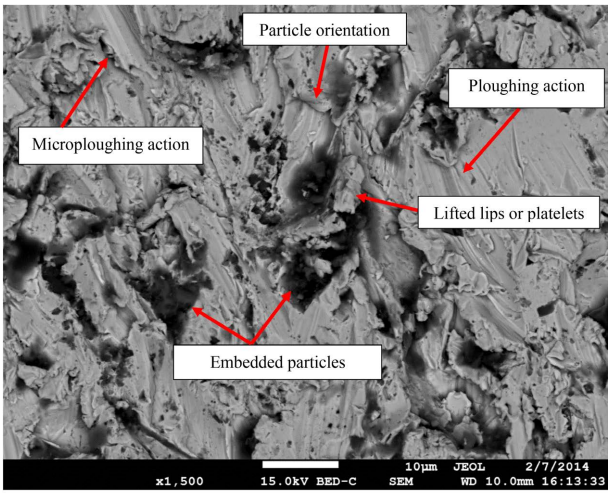

(c)

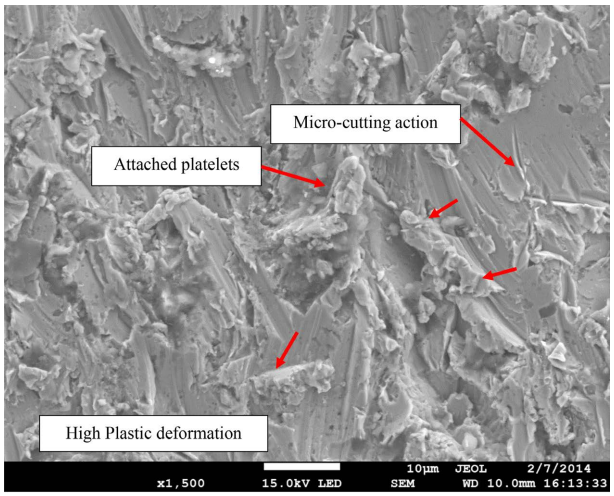

(d)

Figure 2. Erosion damage on AISI 304 by alumina particles at 30˚. (a) BED detector 500×; (b) LED detector 500×; (c) BED detector 1500×; (d) LED detector 1500×.

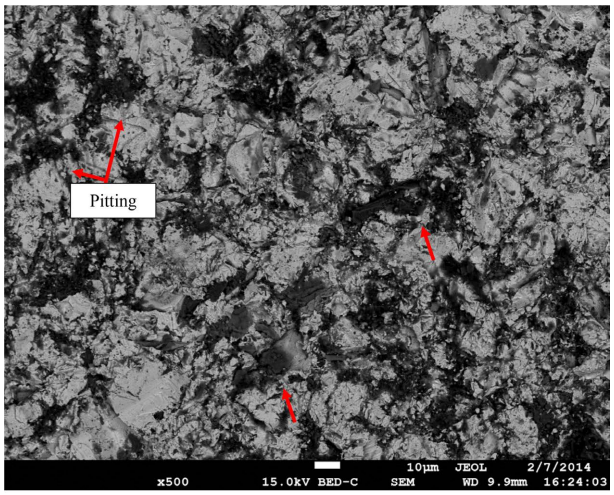

(a)

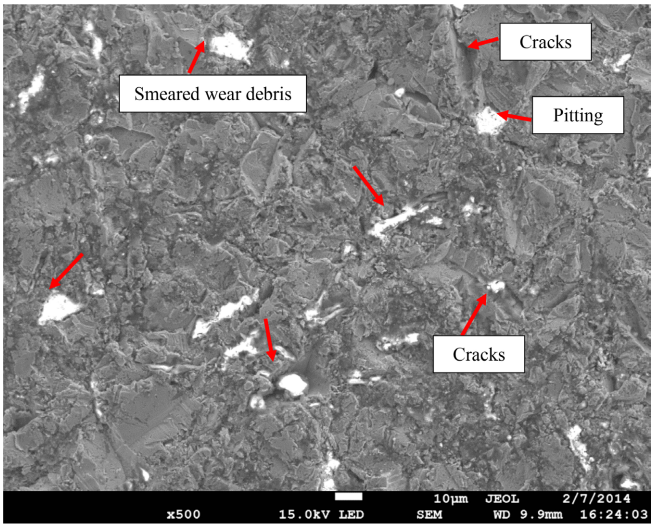
Cracks
Smeared wear debris
Pitting
Cracks
x500 15.0kV LED SEM WD 9.9mm 16:24:03
10μm JEOL 2/7/2014

(b)

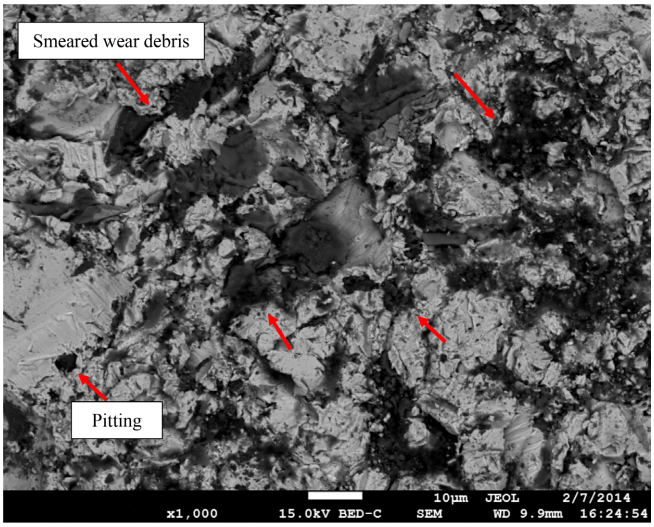
Smeared wear debris
Pitting
x1,000 15.0kV BED-C SEM WD 9.9mm 16:24:54
10μm JEOL 2/7/2014

(c)

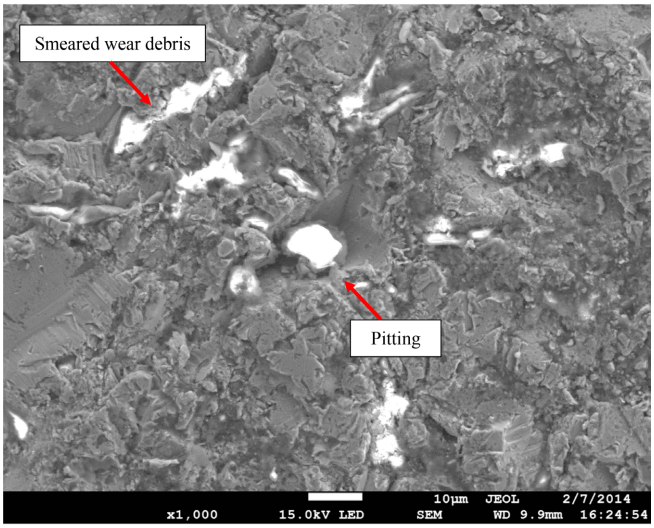
Smeared wear debris
Pitting
x1,000 15.0kV LED SEM WD 9.9mm 16:24:54
10μm JEOL 2/7/2014

(d)

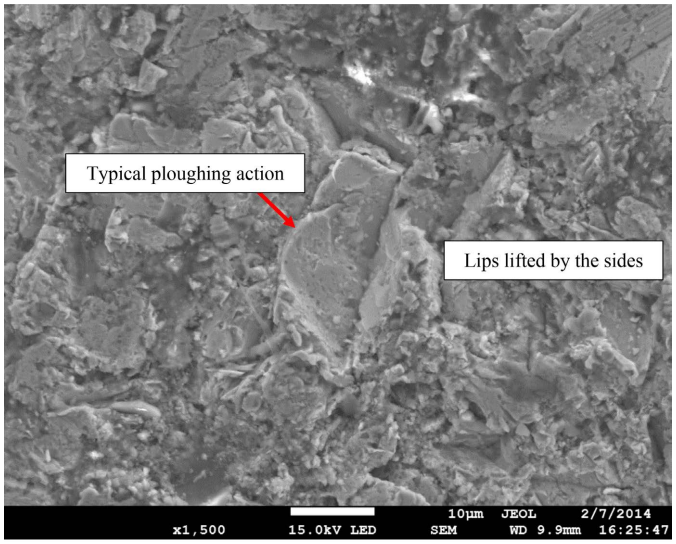

(e)

Figure 3. Erosion damage on AISI 304 by alumina particles at 90˚. (a) BED detector 500×; (b) LED detector 500×; (c) BED detector 1000×; (d) LED detector 1000×; (e) LED detector 1500×.

3.2. Volume Loss and Total Erosion Value

The volume loss (mm^3) was obtained by dividing the mass loss (g) by the density of stainless steel AISI 304 (8.0 g/cm^3). Two tests were conducted for each incident angle and an average volume loss (mm^3) and standard deviation were acquired. The volume loss (mm^3) progressively increased from 2 min to 10 min test, **Figure 4(b)**. The maximum erosion rates were achieved at 30˚ whereas the lowest wear damage was observed at 90˚. This material exhibited a typical ductile behaviour in erosion studies, showing its maximum erosion wear at oblique incident angles (**Figure 6**) [15]-[17]. It related well with the wear mechanisms observed at 30˚, where high plastic deformation on the surfaces was characterized by material displacement due to microploughing, micromachining and cutting actions inflicted by erodent particles sliding on the surfaces. These were relevant to cause intense wear. The low erosion rates at 90˚, were occasioned by the smeared wear debris, flattened platelets, and pits filled by particle or material fragmentations, which led to a decrease in material removal and, therefore, the mass loss. It was interesting to notice that the results at 45˚ and 60˚ were quite close; the volume loss at 60˚ after 10 min, was slightly greater than that seen at 45˚. In addition, the total erosion rates (mm^3/g) were calculated and the results are presented in **Figure 5**. These were obtained by dividing the volume loss (mm^3) by the total mass of particles (g) that stroke the surface after 10 min as specified in ASTM G76. Finally, a comparison among AISI 304 stainless steel (annealed condition), AISI 1018 steel (annealing at 870˚C - 910˚C, slow furnace cooling) and AISI 420 stainless steel (tempered at 600˚C - 750˚C, fast oil cooling) carried out. These three materials were tested under identical testing conditions. In this particular case, AISI 304 demonstrated the highest erosion rates at all impact angles, followed by AISI 1018 at 30˚, 45˚

and 60˚ and the performance was different at 90˚ where AISI 420 steel had more serious erosion damage. The AISI 420 stainless steel presented a better erosion resistance at 30˚, 45˚ and 60˚ than AISI 304 and AISI 1018, due to its higher tensile strength (roughly 1056 MPa) and greater capacity to deform plastically in a permanent form, suffering lower damage. However, the abrasive particles eroded the AISI 420 surfaces at 90˚ in a more intense mode, causing a higher erosion rate than that observed with AISI 1018 steel. It related to the martensitic structure of AISI 420 steel, which behaved in a brittle manner in this particular incident angle, thus the erodent particles, caused a pronounced pitting action and fracture of the adjacent lips, leading to an increase in the material removal from the surface at normal incidence.

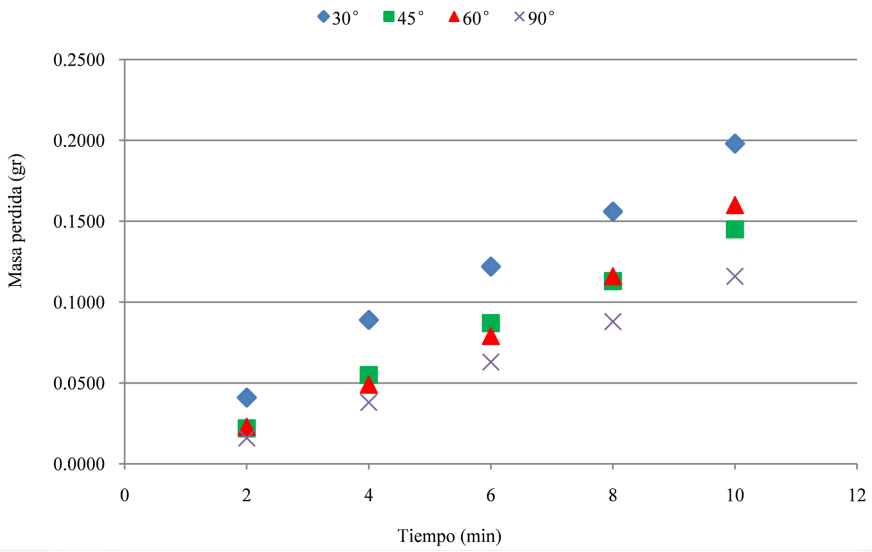

(a)

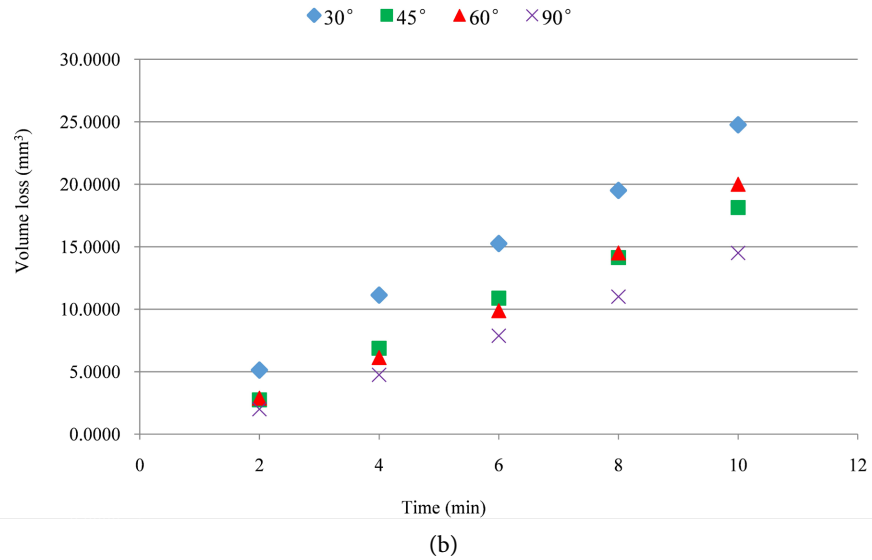

(b)

Figure 4. Erosion Graphs. (a) Mass loss (g) vs time (min); (b) volume loss (mm³) vs time (min).

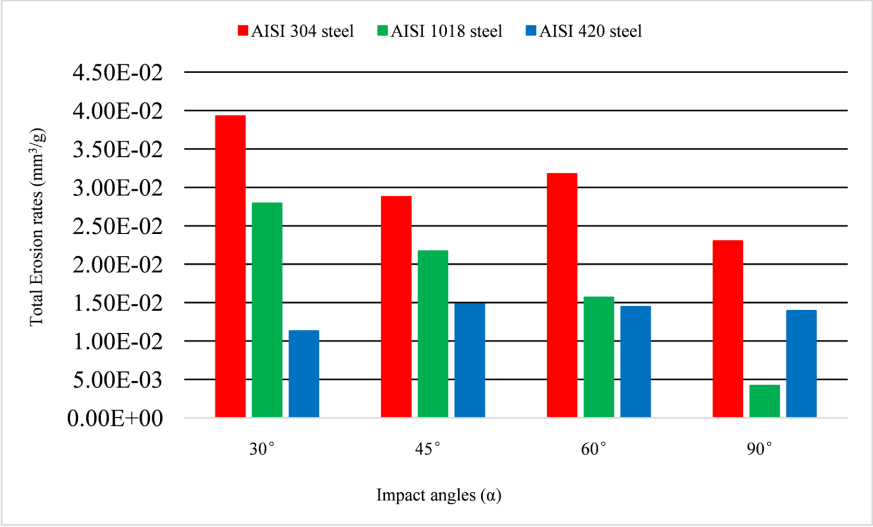

Figure 5. Total erosion value (mm^3/g) vs impact angle (α).

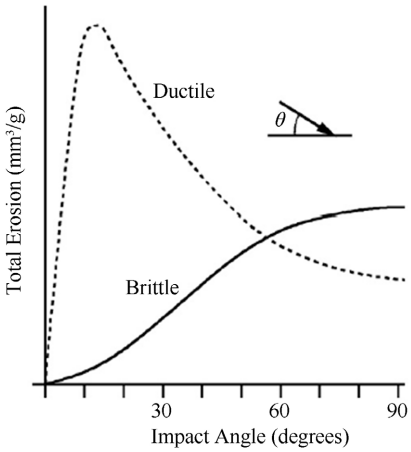

Figure 6. Graph of the typical material behaviour in erosion studies [15].

4. Conclusions

The results presented in the discussion section allow some conclusions to be drawn in relation to the erosion performance of AISI 304 stainless steel against the impact action of alumina particles.

1) The AISI 304 stainless steel showed its maximum erosion rates at 30˚ as alumina was employed to conduct the erosion tests. AISI 304 exhibited typical ductile behaviour in these particular testing conditions, based on other erosion studies.

2) SEM images were used to identify the wear mechanisms. Typical wear modes such as micro-cutting, micro-ploughing with displaced material, and at the end of particle trajectories, lifted lips or platelets and irregular indentations observed with alumina particles at 30˚ (low incident angle) and 90˚ (high incident angle). In addition, pits filled with smeared wear debris, or particle fragments and flattened deformed material were observed in eroded surfaces at 90˚ with both detectors.

3) AISI 304 stainless steel showed higher erosion rates than those reached with

AISI 1018 and AISI 420 stainless steel. This material presented more damage than the other two tested steels. These results were similar to those obtained in other research works but using SiC erodent particles. Mechanical properties such as tensile strength, ductility, hardness and toughness played a significant role in understanding the ductile behaviour in erosion studies.

It would be interesting to conduct more erosion tests on other stainless steels and steels used for the manufacture of pipes that transport gas and oil, in order to compare their performance and have a classification based on their erosion resistance. Other testing conditions, such as different incidence angles, particle velocities, particle fluxes and abrasive particles, could be used to determine their erosion resistance under different operating parameters. Steel alloys are quite interesting to continue learning about their behaviour under this wear process due to their high hardness and ductility.

Acknowledgements

We recognize the experimental support of the Mechanics Laboratory of the Faculty of Mechanical and Electrical Engineering of the Universidad Veracruzana in Poza Rica and the Center for Nanosciences and Micro and Nanotechnology of the National Polytechnic Institute (CNMN-IPN) to complete the present work.

Author's Contribution Statement

All persons who meet authorship criteria are listed as authors, and all authors certify that they have participated sufficiently in the work to take public responsibility for the content, including participation in the concept, design, analysis, writing, or revision of the manuscript. Furthermore, each author certifies the present manuscript is original and has been developed in the Faculty of Mechanical and Electrical Engineering by all the authors included in the paper. The paper does not contain material that has been published previously.

C. M. Calderón-Ramón, H. D. López-Calderón, C. Cortez-Domínguez: Conceptualization, Methodology, Supervision, **V. Velázquez-Martínez, G. Juárez-Morales, J.A. Chagoya-Ramírez, P. Ramirez-Sánchez**: Data curation, Visualization, Validation, **S. M. Sánchez-Yáñez, J. Calderón-Sánchez, J.E. López-Calderón**: Writing—Original draft preparation, Writing—Reviewing and Editing.

Conflicts of Interest

The authors declared no potential conflicts of interest with respect to the research, authorship, and/or publication of this article.

References

[1] Laguna-Camacho, J.R., Villagrán-Villegas, L.Y., Martínez-García, H., Juárez-Morales, G., Cruz-Orduña, M.I., Vite-Torres, M., Ríos-Velasco, L. and Hernández-Romero, I. (2016) A Study of the Wear Damage on Gas Turbine Blades. *Wear*, **61**, 88-99. https://doi.org/10.1016/j.engfailanal.2015.10.002

[2] Camacho, J., Lewis, R. and Dwyer-Joyce, R.S. (2009) Solid Particle Erosion Caused

by Rice Grains. *Wear*, **267**, 223-232. https://doi.org/10.1016/j.wear.2008.12.034

[3] Morrison, C.T., Scattergood, R.O. and Routbort, J.L. (1986) Erosion of 304 Stainless Steel. *Wear*, **111**, 1-13. https://doi.org/10.1016/0043-1648(86)90071-2

[4] Foley, T. and Levy, A. (1983) The Erosion of Heat-Treated Steels. *Wear*, **91**, 45-64. https://doi.org/10.1016/0043-1648(83)90107-2

[5] Tilly, G.P. (1969) Sand Erosion of Metals and Plastics: A Brief Review. *Wear*, **14**, 241-248. https://doi.org/10.1016/0043-1648(69)90048-9

[6] Goretta, K.C., Arroyo, R.C., Wu, C.T. and Routbort, J.L. (1991) Erosion of Work-Hardened Copper, Nickel and 304 Stainless Steel. *Wear*, **147**, 145-154. https://doi.org/10.1016/0043-1648(91)90125-E

[7] Singh, T., Tiwari, S.N. and Sundararajan, G. (1991) Room Temperature Erosion Behavior of 304, 316 and 410 Stainless Steels. *Wear*, **145**, 77-100. https://doi.org/10.1016/0043-1648(91)90240-U

[8] Shayler, P.J. and Yee, K.H. (1984) Erosion of AISI 303 Steel by Fine (about 5 μm and about 50 μm) Ash Particles. *Wear*, **98**, 127-140. https://doi.org/10.1016/0043-1648(84)90222-9

[9] ASTM Standard G76-95 (1995) Standard Practice for Conducting Erosion Tests by Solid Particle Impingement Using Gas Jets. https://www.astm.org/g0076-95.html

[10] Laguna-Camacho, J.R., Hernández-Romero, I., Escalante-Martínez, J.E., Márquez-Vera, C.A., Galván-López, J.L., Méndez-Méndez, J.V., Arzate-Vázquez, I. and Andraca-Adame, J.A. (2015) Erosion Wear of AISI 420 Stainless Steel Caused by Walnut Shell Particles. *Transactions of the Indian Institute of Metals*, **68**, 633-647. https://doi.org/10.1007/s12666-014-0493-5

[11] Liebhard, M. and Levy, A. (1991) The Effect of Erodent Particle Characteristics on the Erosion of Metals. *Wear*, **151**, 381-390. https://doi.org/10.1016/0043-1648(91)90263-T

[12] Huttunen-Saarivirta, E., Kinnunen, H., Tuiremo, J., Uusitalo, M. and Antonov, M. (2014) Erosive Wear of Boiler Steels by Sand and Ash. *Wear*, **317**, 213-224. https://doi.org/10.1016/j.wear.2014.06.007

[13] Hutchings, I.M. and Winter, R.E. (1974) Particle Erosion of Ductile Metals: A Mechanism of Material Removal. *Wear*, **27**, 121-128. https://doi.org/10.1016/0043-1648(74)90091-X

[14] Finnie, I., Levy, A. and Mcfadden, D. (1979) Fundamental Mechanisms of the Erosive Wear of Ductile Metals by Solid Particles. https://doi.org/10.1520/STP35794S

[15] Hutchings, I.M. (1992) Tribology: Friction and Wear of Engineering Materials. 1st Edition, Butterworth-Heinemann.

[16] Laguna-Camacho, J.R., Marquina-Chávez A., Méndez-Méndez J.V., Vite-Torres M. and Gallardo-Hernández, E. A. (2013) Solid Particle Erosion of AISI 304, 316 and 420 Stainless Steels. *Wear*, **301**, 398-405. https://doi.org/10.1016/j.wear.2012.12.047

[17] Laguna-Camacho, J.R., Martínez-García, H., Escamilla-Rodríguez, F., Alarcón-Rosas, C., Calderón-Ramón, C.M., Ríos-Velasco, L., Pelcastre-Lozano, M., Casados-Sánchez, A. and González-Gómez, M. (2015) Erosion Behavior of AISI 6061-T6. *Journal of Surface Engineered Materials and Advanced Technology*, **5**, 136-146. http://dx.doi.org/10.4236/jsemat.2015.53015